Section A-Research paper

ULTRASONIC ASSISTED SYNTHESIS OF CHALCONE AND PYRAZOLINE DERIVATIVE, DFT CALCULATIONS AND THEIR BIOLOGICAL STUDIES

S. Prabha[1,*]

[1]*Dr. S. Prabha, Asst. Prof, Dept. of Chemistry, Govt. Arts College, Chidambaram, Tamilnadu, Inia-608102.*

HI G H L I G H T S

- By adopting Ultrasonic energy, a chalcone compound (**1**) and its pyrazoline derivative (**2**) have been synthesized with low time of reaction.
- They were confirmed by their UV, IR and NMR spectral data.
- The DFT calculations were carried out and the results are compared with experimental and literature values.
- The antimicrobial activities were carried out and showed better activities.
- The anti-inflammatory activities also performed.

Abstract

By utilizing ultrasonic assisted synthetic method, *(E)*-3-(4-nitrophenyl)-1-(m-tolyl)prop-2-en-1-one (**1**) was synthesised using respective ketones and aldehydes. From the compound (**1**), a pyrazoline derivative (**2**) was prepared by cyclization reaction using the same ultrasonic method. These compounds **1** and **2** were characterised by spectral data. Further the DFT analysis were calculated by 6-31G (d ,p)/B3LYP method. From these calculations, the optimized geometries, parameters, vibrational analysis, molecular orbital studies, MEP analysis, dipole moments and Mulliken atomic charges were calculated and compared with literature data. In addition to these studies, the antimicrobial activities of compounds **1** and **2** were screed against different bacterial species and fungal species. Also, the anti-inflammatory activities were performed for such present compounds.

*Corresponding Author E-mail : drsprabhacdm@gmail.com

Telephone : +91 9486717195

GRAPHICAL ABSTRACT:

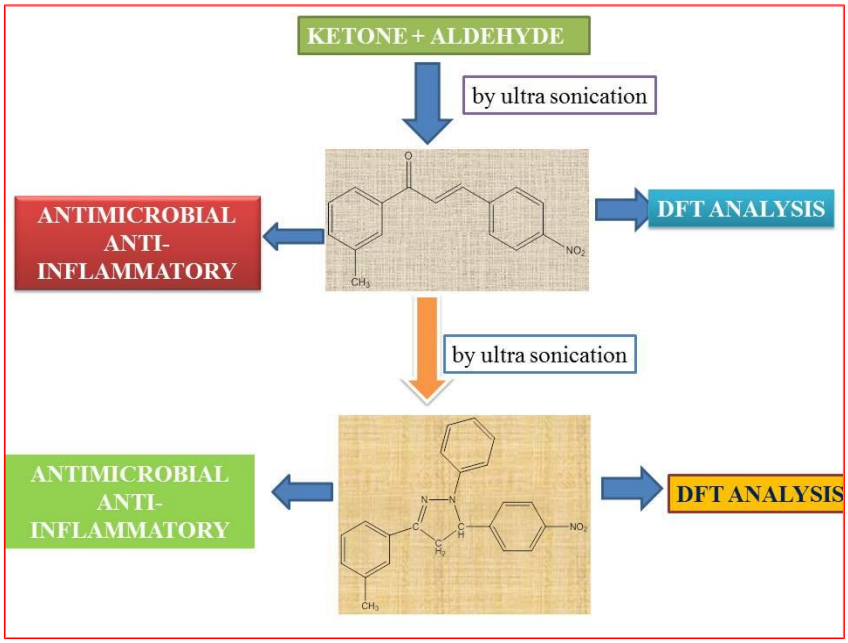

Key words: *Chalcone, pyrazloine, Ultrsonic method, DFT analysis, antimicrobial studies and Anti-inflammatoty activity*

1. Introduction

The chalcone and pyrazoline moieties present are important classes of compounds widely used as building blocks for biologically active compounds and they are considered promising candidates for antifungal drugs. Chalcones have been extensively studied for their broad spectrum of activities as anti-inflammatory [1], antifungal [2,3], antibacterial [4], antioxidant [5], antimalarial [6,7] and antitumor [8,9] agents. Chalcones possesses acceptor and donor groups, which enhance their importance in various fields. Chalcone derivatives are promising compounds to be developed as their chromophore absorbs in the UV region from Sunscreen Agent. The non-linear optical (NLO) properties of conjugated organic compounds have been the major focus of various computational and experimental studies because of their promising applications in photonics and optoelectronics, integrated optics, photophysical, high-speed optical communications, optical data processing, and storage [10,11]. The chalcone compounds have high significance because of their excellent NLO properties [12]. Chalcones are intramolecular charge transfer molecules, which allow one to design them based on the above design criteria. The pyrazole ring is present at the heart in some of the important drugs like celebrex, ionazlac, rimonabant, difenamizole, etc. The wide range of biological activities associated with pyrazole and its derivatives made them popular synthetic targets. Further to the well-known biological activities, pyrazole derivatives substituted with

electron donor and acceptor groups exhibit considerable nonlinear optical properties [13-15]. In the literature, Zhao et al. reported density functional calculations and NBO for 1N-phenyl-3(3,4-dichlorophenyl)-5-phenyl-2-pyrazoline [16]. Experimental and density functional theory calculations have been carried out by Saminathan et al. for pyrazoline fused thiocyanoethanones [17]. In this work, the structural properties and vibrational frequencies have been investigated. The geometries and normal modes of vibrations obtained from DFT calculations are in good agreement with the experimental data. The first hyperpolarizabilities, NBO and HOMO, LUMO analyses of the said molecule have been computed using quantum mechanical calculations. In this paper we describe the synthesis and characterization of chalcone and pyrazoline derivative, containing the *meta*-methyl and *para*-nitro in their structures. These compounds have been utilized to study their DFT calculations including molecular structure, charges, HOMO-LUMO energies, MEP surface dipole moment, polarizability, and first hyperpolarizability. In addition, the antimicrobial and anti-inflammatory activities are performed.

2. Experimental

2.1. Materials and methods

All chemicals were purchased commercially and used without prior purification. Melting points were determined in open capillary tube and were uncorrected. Elemental analyzes were carried out on Variomicro V2.2.0 CHN analyzer. FT-IR spectrum of title compounds were recorded on a Shimadzu FTIR spectrophotometer in the range 400–4000 cm^{-1} using the KBr pellets. The proton and carbon NMR spectra were recorded on a BRUKER AVANCE III 500MHz NMR spectrometer using $CDC1_3$ as solvent. Chemical shifts were reported in ppm. Tetramethylsilane (TMS) was used as internal reference for all NMR spectra, with chemical shifts reported in units (parts per million) relative to the standard. ^{1}H NMR signal patterns are indicated as singlet (*s*), doublet (*d*), doublet of doublet (*dd*), triplet (*t*), quartet (*q*) and multiplet (*m*). The FT-IR and NMR spectra were recorded at Department of Chemistry, Annamalai University, Tamil Nadu.

2.2 Synthesis of compounds

2.2.1 Synthesis of *(E)*-3-(4-nitrophenyl)-1-(m-tolyl)prop-2-en-1-one (1)

Equimolar amount of1-(*m*-tolyl)ethanone (2.5 mmol) and 4-nitrobenzaldehyde (2.5 mmol) with absolute ethanol (5 mL), and 40 % sodium hydroxide (20 mmol diluted up to 2 mL) were taken in a 100ml conical flask. The mixture was then exposed to ultrasound irradiation at room temperature [18] for 2 min as shown in **Scheme-1**. The reaction was monitored by thin-layer chromatography (eluent 20:80: ethyl acetate: hexane). The reaction mixture was quenched by pouring on ice. After this, the resulting mixture was acidified by using dilute HCl and the resulting precipitate was then filtered and dried to give the desired product. The obtained product was recrystallized from hot ethanol. The synthesized pure products were characterized by UV, FT-IR, ^{1}HNMR, ^{13}C NMR and Mass analytical methods.

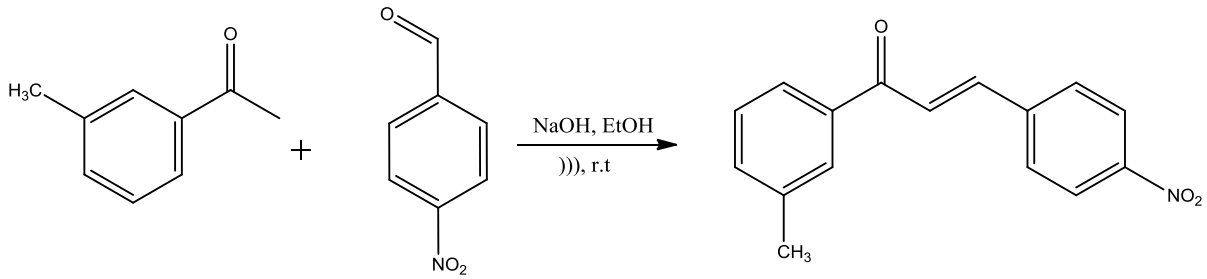

Scheme-1 : Synthesis of chalcone (1)

2.2.2 Synthesis of 5-(4-nitrophenyl)-4,5-dihydro^{-1}-phenyl-3-*m*-tolyl-1*H*-pyrazole (2)

A mixture of (*E*)-3-(4-nitrophenyl)-1-(*m*-tolyl)prop-2-en-1-one (2.5mmol) with phenylhydrazine (2.5mmol) in ethanol and glacial acetic acid were taken in a 100ml conical flask. The reaction flask was kept at center of the ultrasonic bath to get maximum ultrasound energy and sonicated [18] at room temperature for 20-25min as shown in **Scheme-2**. The completion of the reaction was monitored continuously by TLC. After completion of the reaction, the mixture was poured into crushed ice and kept overnight. The precipitated formed was separated by filtration and died well then recrystallized using hot ethanol to yield pale range colored crystals.

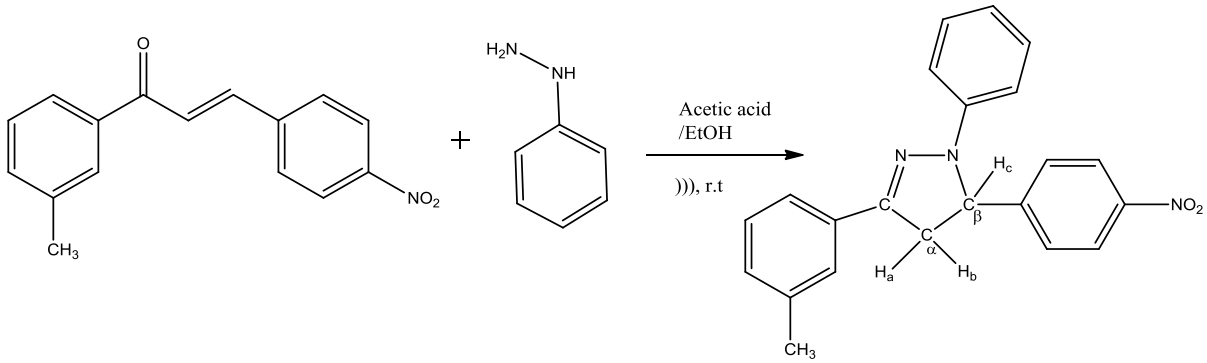

Scheme-2 : Synthesis of pyrazoline (2)

2.3. Computational study.

Geometry optimizations were carried out according to density functional theory using B3LYP/6-31G(d,p) basis set in the Gaussian-09 package. The polarizabilities and hyperpolarizabilities have been derived from the DFT optimized structure by using finite discipline technique using the B3LYP/6-31 G basis set, while the NBO calculations were carried out using the premise set B3LYP/6-31 G (d,p) available in Gaussian-09.

3. Results and Discussion

3.1 Spectral analysis

The physical and spectral measurements of the synthesised compounds are given below.

3.1.1 Spectral analysis of *(E)-3-(4-nitrophenyl)-1-(m-tolyl)prop-2-en-1-one* (1)

Yield 82%; mp 106-107 ˚C; m/z 296; UV (CH_3OH, λ_{max}^{nm}) 299.00, IR (KBr, νcm^{-1}) 1656.85 (CO), 1213.23 (CH_{ip}), 910.40 (CH_{op}), 1026.13 ($CH{=}CH_{op}$), 497.63 ($C{=}C_{op}$). ^1H NMR (500 MHz, $CDCl_3$, δ/ppm) d 7.723(1H, *d*, J = 15 Hz), 7.739 (1H, *d*, J = 15 Hz), 6.920–

7.842 (9H,overlapping m, ArH); ^{13}C-NMR (125 MHz, $CDCl_3$, δ/ppm) 125.645 (C_α), 142.847 (C_β), 189.682(CO), 123.212-141.054 (Ar. Carbons). Anal. Calcd. for $C_{16}H_{13}NO_3$.

3.1.2 Spectral analysis of 5-(4-nitrophenyl)-4,5-dihydro^{-1}-phenyl-3-*m*-tolyl^{-}1*H*-pyrazole (2)

UV λ_{max}(nm): 315.80; IR νcm^{-1}: 3442.94 (N-H str.), 1620.21 (C=N), 2918.30 (ali. -CH str.), 823.60 (N-N); ^{1}H NMRδ(ppm): 3.154(H_a, 1H-*dd*)ppm, 3.843(H_b, 1H-*dd*)ppm, 5.269(H_c, 1H-*d*)ppm, 6.802-7.826(*m*, Aromatic protons)ppm, ^{13}C NMR δ(ppm):146.916(C=N)ppm,43.722(Cα)ppm,64.241(C_β)ppm,29.70340(C-CH_3)ppm, m.p. 131-132°C; Molecular Formula: $C_{22}H_{19}N_3O_2$.

3.2 Geometrical optimization

The entire molecular geometries of **1** and **2** were optimized by DFT method. The optimization results of compounds **1** and **2** are presented in **Fig. 1** and **Table 1**. To the best of our knowledge, exact experimental data on the geometrical parameters of compounds **1** and **2** are not available in the literature.

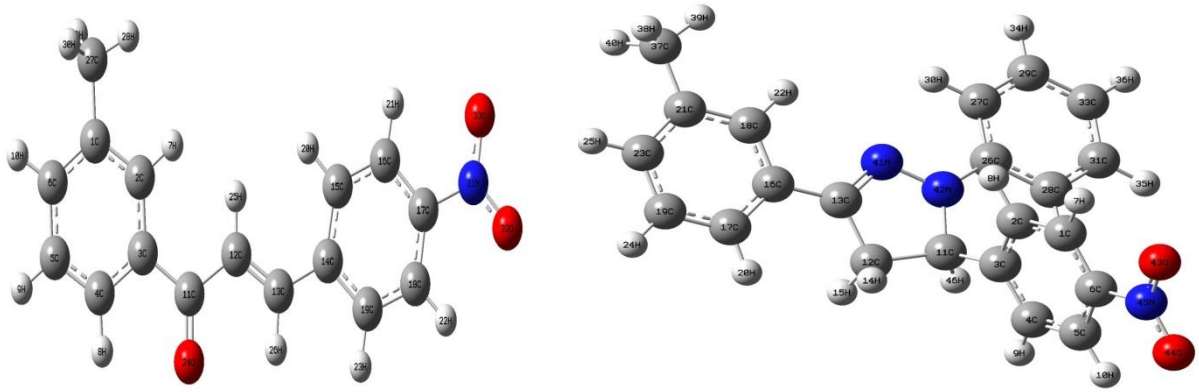

Chalcone (1) **Pyrazoline (2)**

Figure 1: Optimized structures of compounds **1** and **2**.

Table 1: Selected bond lengths, bond angles and dihedral angles of compounds **1** and **2**

Bond lengths				Bond angles				Dihedral angles			
Chalcone		Pyrazoline		Chalcone		Pyrazoline		Chalcone		Pyrazoline	
Position	Length (A°)	Position	Length (A°)	Position	Angles (°)	Position	Angles (°)	Position	Dihedral angles (°)	Position	Dihedral angles (°)
C2-H7	1.084	C3-C2	1.406	C2-C3-C11	123.39	H10-C5-C6	119.59	C3-C11-C12-C13	177.33	C3-C11-N42-C26	72.37
C4-H8	1.084	C11-C3	1.524	C3-C11-C12	120.02	C11-C3-C2	120.96	C4-C3-C11-C12	171.54	C13-N41-N42-C11	3.36
C12-H25	1.083	C12-C11	1.565	H7-C2-C1	117.98	C12-C13-C16	124.86	C11-C12-C13-C14	179.19	C13-C16-C17-C19	180.24
C13-H26	1.089	N42-C11	1.485	C11-C12-C13	120.3	H14-C12-C11	111.5	C12-C13-C14-C19	178.87	H14-C12-C13-C16	55.29
C15-H20	1.084	C12-C13	1.524	C12-C13-C14	127.47	H15-C12-C13	111.01	C13-C14-C19-C18	179.95	C16-C13-N41-N42	179.17
C19-H23	1.085	C16-C3	1.460	C12-C11-O24	119.97	C18-C16-C13	120.64	C14-C19-C18-C17	0.03	H20-C17-C19-C23	179.93
C27-H28	1.094	N41-C13	1.306	C13-C14-C19	118.44	H20-C17-C16	120.34	H20-C15-C16-C17	180.16	C28-C26-N42-C11	4.11
C27-H29	1.097	C12-H14	1.094	C14-C19-C18	121.32	H24-C19-C17	119.68	H21-C16-C17-N31	0.05	N41-C11-C26-N42	6.19
C27-H30	1.097	C12-H15	1.097	C15-C16-C17	118.93	H25-C23-C19	119.89	O24-C3-C12-C11	0.59	O44-N45-C6-C1	180.37
O24-C11	1.257	C16-C17	1.408	C16-C17-C18	121.81	C27-C26-N42	120.3	H25-C12-C13-C14	0.27	H46-C11-C3-C2	154.91
C13-C12	1.351	N42-C26	1.402	C17-C18-C19	118.62	H30-C27-C26	119.01	H26-C13-C14-C15	178.63	C17-C16-C13-N41	178.42
C11-C12	1.483	N41-N42	1.388	C18-C17-N31	119.16	H32-C28-C26	120.61	O32-N31-C17-C16	180.07	C18-C16-C13-C12	179.69
N31-C17	1.463	C11-H46	1.096	H25-C12-C13	121.14	H34-C29-C27	119.03	O33-C17-O32-N31	0.01	C27-C26-N42-C11	175.706
O32-N31	1.265	C1-C6	1.398	H26-C13-C14	116.21	H35-C31-C28	119.03			C28-C26-N41-N42	176.876
O33-N31	1.266	C6-C5	1.397	H28-C27-H30	107.7	H36-C33-C29	120.52			N42-C11-C3-C4	-149.85
C13-C14	1.463	C2-C1	1.394			C37-C21-C18	120.93			C12-C11-C3-C2	-81.703
C11-C12	1.483	C31-C28	1.398			N41-N42-C26	120.84				
C3-C11	1.492	C27-C29	1.394			N45-C6-C1	119.12				
C18-C19	1.392	C4-C3	1.406			H46-C11-N42	109.55				
C15-C16	1.390										
C17-C18	1.397										
C16-C17	1.400										
C1-C6	1.406										
C3-C4	1.407										
C4-C5	1.394										

In unsubstitted benzene, the bond lengths are nearly similar between. If a substituent may be either electron withdrawing or electron donating type which alters the bond length [19]. In the present study, the bond lengths in aromatic carbons are calculated in the range of 1.39-149 Å for B3LYP level. The aliphatic C12=C13 bond length is calculated at 1.35 Å, The aromatic C-H bond lengths are calculated in the range of 1.08-1.09 Å for chalcone. The carbonyl group bond length is calculated at 1.25 Å. The vinyl C-H lengths like C12-H25 and C13-H26 are calculated at ~1.08 Å. In case of pyrazoline, the aromatic C=C and C-H bond lengths are calculated in the range of 1.39 – 1.45 Å and 1.08 – 1.09 Å respectively. There are two C-N bonds are observed in pyrazoline, one is single bonded another one is double bonded. In the present calculations C13-N41 bond length was calculated at 1.306 Å and C11-N42 was calculated at 1.484 Å. It clearly denotes that the low bond length in C13=N41 was exhibited by double bond character and the higher bond length between C11-N42 implies the single bond character. The N41-N42 bond length was calculated at ~1.38 Å. The dihedral angle was calculated for C11-C12-C13-C14 at 179° and it clearly implies that chalcone molecule has been exhibited in *E*-configuration. All bond lengths and angles are within the normal ranges and compared with previously reported structures of chalcones [20–22].

The rings of *m*-methyl substituted phenyl-pyrazole that lies in the same plane which are evidenced from dihedral angles calculated for C17-C16-C13-N41and C18-C16-C13-C12 at ~179°. But the dihedral angles for N42-C11-C3-C4 (-149.852°) and C12-C11-C3-C2 (-81.7031°) are calculated at lower values and it clearly implies that the *p*-nitro substituted phenyl-pyrazole rings are not in the same plane. All the geometric papameters were agreed with previously reported pyrazolines [23-25].

3.3. Vibrational analysis

The compound **1** has C1 symmetry. In this compound 1, 33 atoms are present and have 93 fundamental vibrational modes which are by B3LYP/6-31G (d, p) level. Some of the selected vibrational frequencies which are occurred experimentally and theoretically are presented in **Table 2**. For chalcones, the stretching vibration for carbonyl group is generally appeared at 1750–1600 cm^{-1} [20]. The present compound **1** possesses the vibrational frequency at 1656 cm^{-1} in experimental IR and theoretically calculated at 1675 cm^{-1}. These frequencies are agreed with previously reported data [21, 22]. The C-H stretching vibrations of aryl groups usually occur above 3000 cm^{-1} [26]. These vibrations were included in the range 3208-3119 cm-1 and a mixed vibration band was experimentally found at 3091 cm^{-1}. In-plane and out-of-plane C-H bending vibrations for aromatic rings and vinyl groups were observed at 1213, 910, 812, 692 cm^{-1} (Table 4) and calculated at 1210, 915, 818, 706 cm^{-1}. In the previously reported chalcone derivatives, the C=C stretching frequency of the enone fragment was found to be 1592 cm-1 and calculated as 1588 cm^{-1} [21]. The vibration in the name molecule was calculated as 1593 cm-1 and experimentally found as 1580 cm^{-1}. The aromatic C=C stretch vibration of the title compound occurs at 1531 cm^{-1} theoretically given at 1533 cm^{-1}. The out-of-plane bending vibration at 1026 cm^{-1} indicates the *trans* geometry of the alkene. Peaks

resulting from asymmetric and symmetrical methyl stretch modes are generally observed between 2965 and 2880 cm^{-1} [28]. Methyl stretching vibrations calculated in the range of 3013-2891 cm^{-1}. In the FT-IR experiment, the symmetrical stretching vibrational mode of the methyl group was observed at 2920 cm^{-1}. Asymmetric and symmetrical deformations of the methyl group occur in the region of 1465-1440 cm^{-1} and in the region of 1390-1370 cm^{-1}, respectively [28, 29]. In the present case, methyl group deformation mode has been calculated at 1424 $cm^{-1}$and observed at 1406 cm^{-1}. The NO_2 stretching vibrations which are another characteristic vibration mode were observed at 1519 cm^{-1} for asymmetric stretch and 1312 cm^{-1} for symmetric stretch [25]. It is well known that asymmetric vibrations appear at higher frequencies than symmetric ones for nitro group vibrations. These vibrations were assigned at 1490 and 1213 cm^{-1} for experimental and 1474 and 1219 cm^{-1} for B3LYP level, respectively. The experimental and DFT IR spectra of compounds **1** and **2** are displayed in **Fig. 2** and **3** respectively.

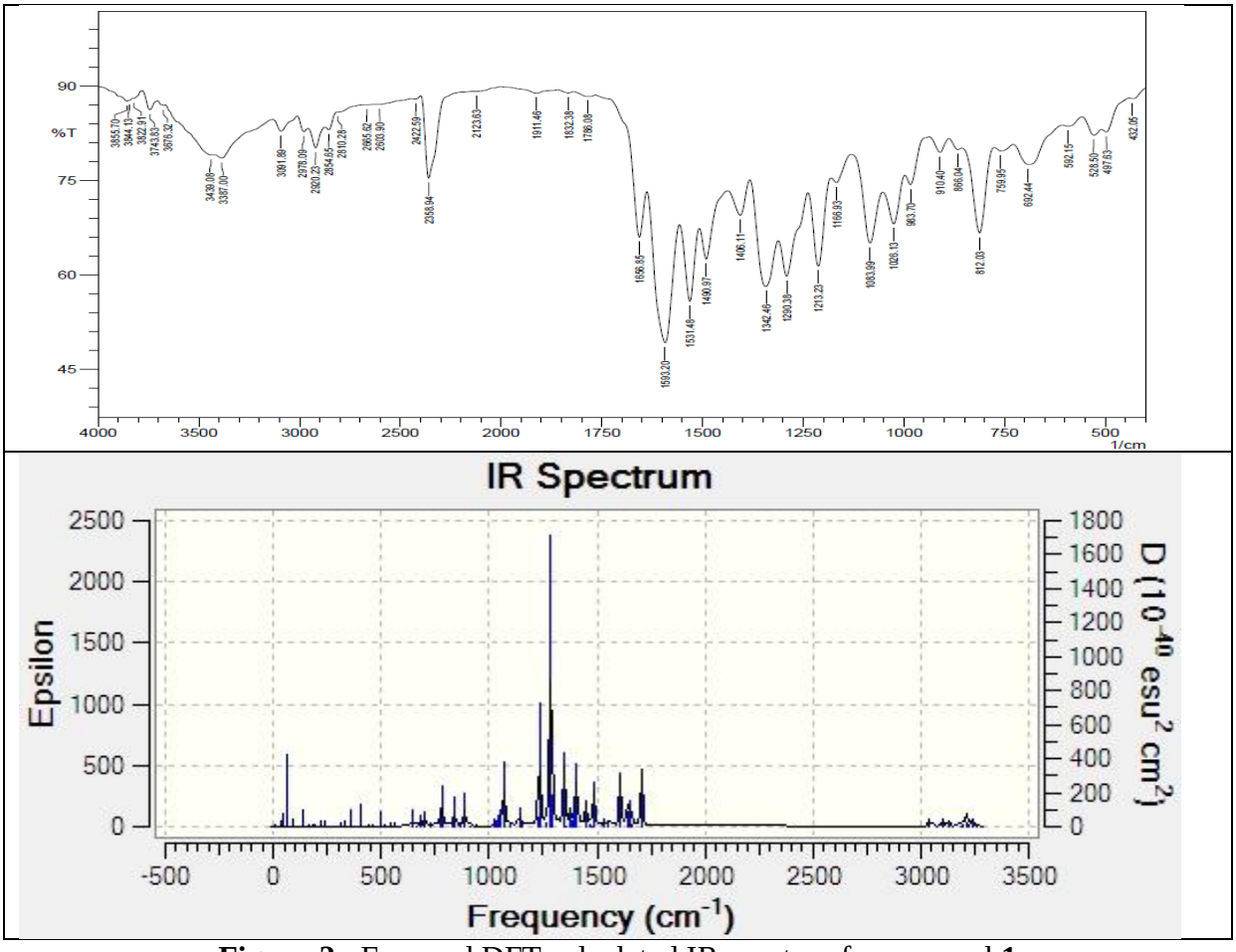

Figure-2 : Exp. and DFT calculated IR spectra of compound **1**

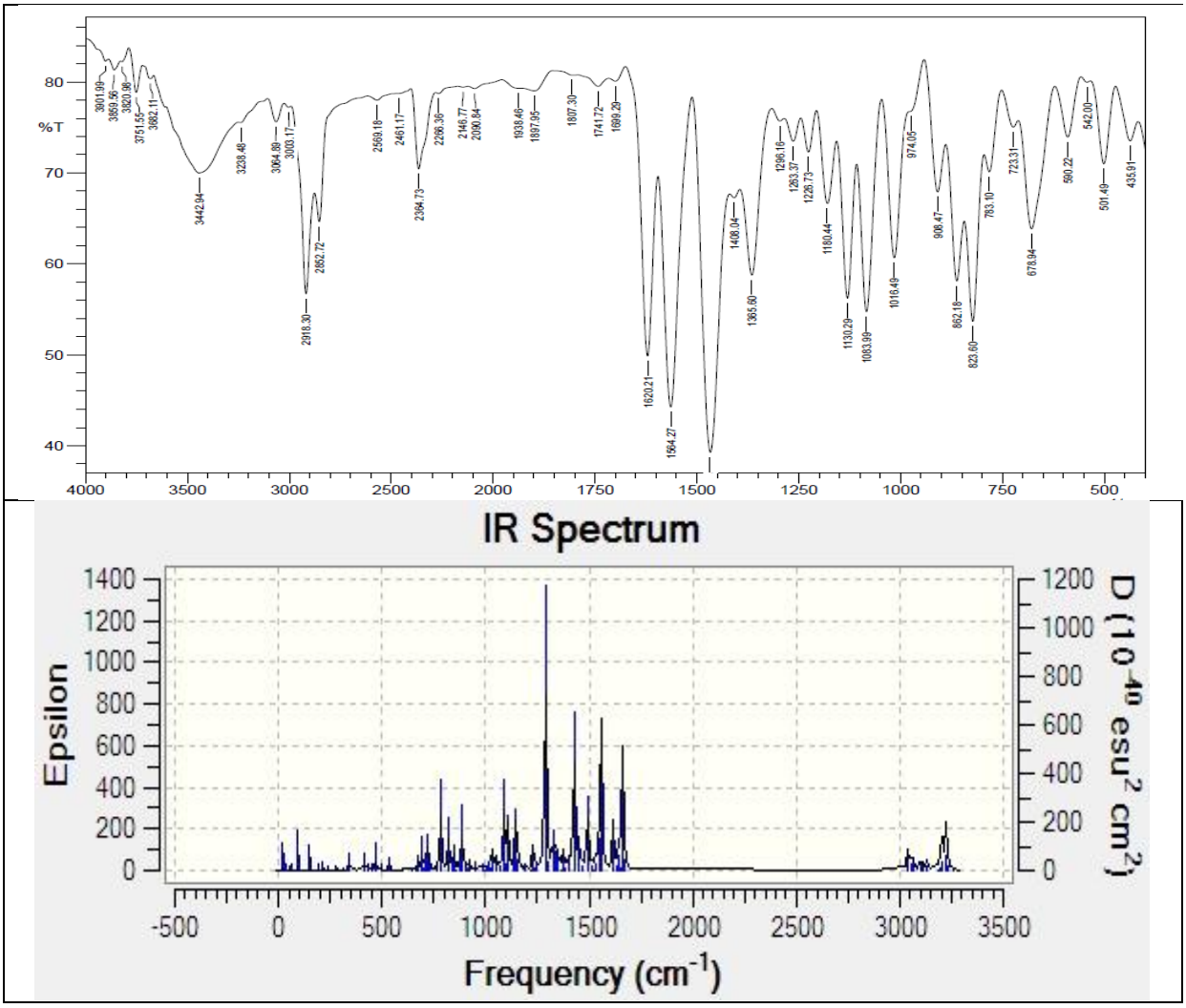

Figure-3 : Exp. and DFT calculated IR spectra of compound **2**

In pyrazoline, the N–H stretching vibration of compounds can be traced around 3450–3150 cm^{-1} in FT-IR Spectra [24]. In present compound, N–H stretching vibration was observed at 3442 cm^{-1}. It has been calculated around 3362 cm^{-1} for title compounds.

The N–H bending vibration was observed at 1408 cm^{-1}, while the calculated peak observed at 1407 cm^{-1}. These bending N–H vibrations are mixed normal modes in which the corresponding C=C stretches are constantly involved. The peaks observed in the range 3003-3067 cm^{-1} were assigned as aromatic C–H stretching vibrations, while the calculated peak was observed ca. 3052-3114 cm^{-1}. Udaya Sri et al.[30] had observed the $–CH_2–$ band at 2922 cm^{-1}in diethyl 1*H*-pyrazole-3,5-dicarboxylate. In this case, the $–CH_2–$ fragment in the pyrazole moiety gives rise to band at 2918 cm^{-1}, whereas calculated band observed ca. 2846 cm^{-1}.

Table-2 : Selected Experimental and DFT calculated IR frequencies of compounds **1** and **2**

Chalcone (1)				**Pyrazoline (2)**			
Experimental frequencies (cm^{-1})	**Calculated (scaled) frequencies (cm^{-1})**	**Calculated IR intensity**	**Assignment**	**Experimental frequencies (cm^{-1})**	**Calculated (scaled) frequencies (cm^{-1})**	**Calculated IR intensity**	**Assignment**
3387	3222.28	11.49	CH str	3442	3362.47	1.97	N-H str
	3208.35	4.72	CH str		3114.43	10.66	C=C str
	3193	17.74	CH str		3098.17	21.73	CH_3 asym
	3173.5	6.36	CH str	3064	3067.9	19.77	C=C str
3091	3163.75	0.04	β-CH str	3003	3052.59	17.7	C=C str
2978	3119.64	11.73	CH_3 asym	2918	2846.41	37.36	ali. C-H-str
2920	3090.95	14.63	CH_3 asym	1620	1663.25	158.83	C=N str
2123	3047.46	19.68	CH_3 sym		1552.45	51.19	CH_3 asym
1656	1675.47	112.43	CO str		1450.9	43.45	NO2 asym
	1592.89	21.01	aro. C=C str	1408	1407.26	9.19	N-H ben
1593	1580.48	71.94	ali.C=C str		1289.03	379.65	NO_2 sym
	1562.3	14.73	CH3 sym		1246.38	9.01	CH_2-def-op
	1558.47	7.8	CH_3 def	1130	1147.83	71.35	ar. C-H def-ip
1531	1533.66	12.53	aro. C=C str	1083	1091.28	102.08	ar. C-H def-ip
	1527.28	1.64	ar. C-H def-ip	1016	1029.43	16.63	C-H-def-op
1490	1474.27	3.48	NO_2 asym	823	822.29	44.53	C-H str, N-N str
	1456.83	70.65	CH def	678	695.21	24.45	C-H-def-op, NO_2 asym-op,
	1454.86	6.68	CH_3 asym	590	596.99	1.8	ar. C-H bend, CH_2- def-ip

1406	1424.54	57.97	CH_3 asym
	1373.01	83.15	CH def-ip
	1357.18	51.12	CH def
1342	1355.06	77.46	CH def
	1307.27	44.81	C=C str
1290	1268.57	96.53	CH def
	1246.91	56.06	CH def, C-N str
1213	1210.79	240.91	CH def-ip
	1101.62	9.08	CH_3 asmy
1026	1056.65	85.71	ali.C=C def
	1049.42	15.39	CH def-ip
	1046.31	24.92	CH def-ip
	1044.16	10.05	CH def-ip
	1036.96	5.75	CH def-ip
963	1035.1	31.05	CH def-ip
	1029.4	29	C=C def
	982.16	0.49	CH def-op
	956.17	4.66	CH def-op
	934.85	0.19	CH def-ip
910	915.02	2.88	CH def-op
812	818.82	15.12	CH def-ip
692	706.04	18.73	CH def-ip
592	645.35	10.3	CH def-ip
528	527.13	1.53	CH def-op
497	494.44	2.93	C=C def

str : stretching; asym : asymmetric stretching; sym :symmetric stretching; def-ip : in-plane bending; def-op : out of plane bending; Scale factor: 0.9608-B3LYP/6-31G(d,p).[31]

3.4 Molecular orbital analysis

The molecular orbitals (MOs) are noticeable quantum chemical factors for the determination of interaction of a molecule with neighbour species and also for characterization of global softness, chemical reactivity, molecule's kinetic stability and hardness [32, 33]. Hence, we performed HOMO-LUMO analysis in order to understand the molecular orbital behaviour of our title compounds. For this reason, HOMO-LUMO analysis of the title compounds calculated using B3LYP/6-31G (d,p) methodology and results are tabulated in Table 3. Pictorial representations of these molecular orbitals are furnished in **Fig. 4**. High HOMO energy levels represent compounds that are good nucleophiles, and low LUMO levels represent compounds that are good electrophiles [34]. The molecular frontier orbital energies are shown in Figure 7. From Figure 6, the values of E-HOMO and E-LUMO are given in Table-. The HOMO-LUMO energy variations (ΔE) for Chalcone and Pyrazoline compounds have been found as 3.644 eV and 2.258 eV respectively and it indicates that there is possible for intramolecular charge-transfer interaction in these molecules. A wide band gap describes the hardness of the molecule, which is related to the non-reactivity of the molecule. The energy difference between HOMO and LUMO correlates with hardness. The greater the energy difference, the higher the hardness of the target molecule. Using the calculated HOMO and LUMO energies, we can obtain electrochemical parameters shown in **Table-3** such as the global electrophilic index is $\omega = \mu 2/2\eta$, the global hardness $\eta = (I-A)/2$, the chemical potential $\mu = -(I+A)/2$ and the electronegativity (χ) is $\chi = (I+A)/2$ and the global softness $\nu = 1/\eta$ was called the global reactivity parameter [35–39].

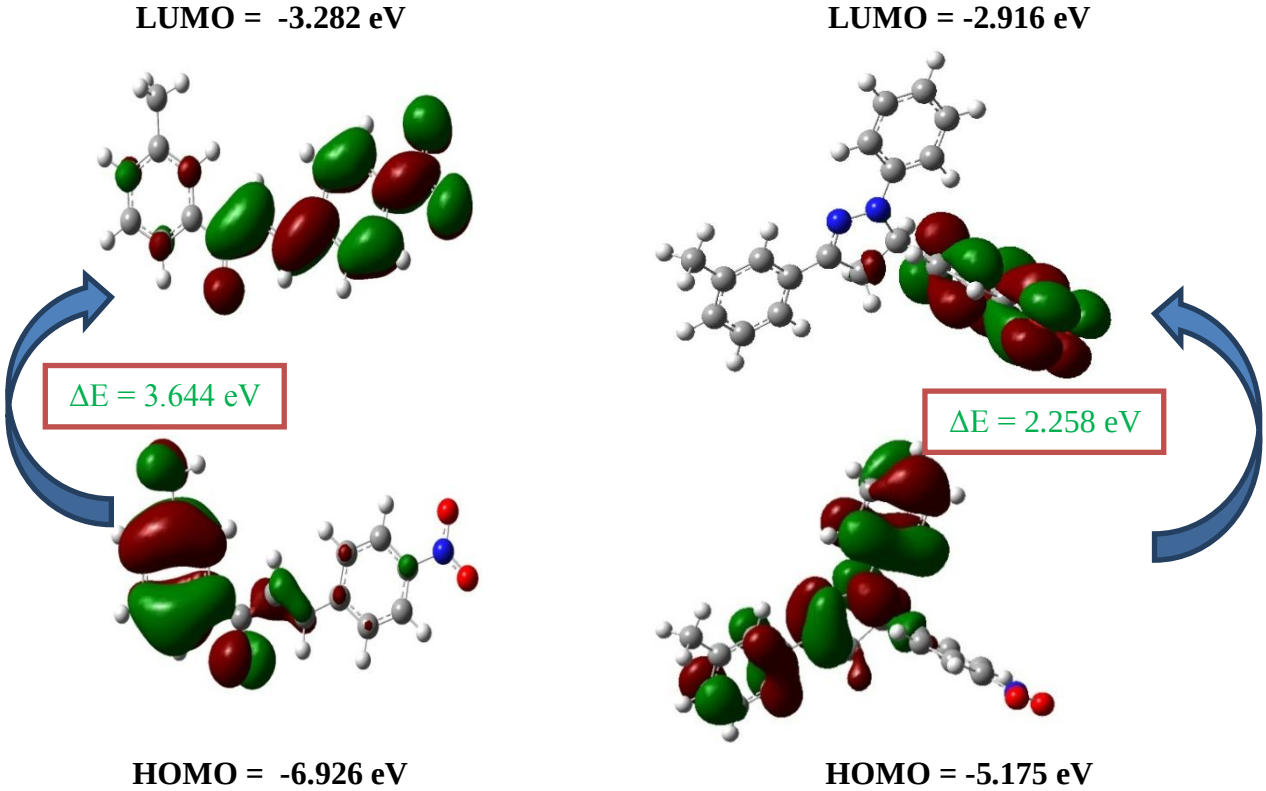

Figure-4 : HOMO-LUMO energies of compounds **1 and 2**

Table-3 : Molecular orbital energies

Parameters	Calculated values	
	Chalcone	**Pyrazoline**
E_{Homo}(a. u)	-6.926	-5.175
E_{Lumo}(a.u)	-3.282	-2.916
Energy gap(a.u)	3.644	2.258
Ionization energy(I)	6.926	5.174
Electron affinity(A)	3.282	2.916
Global hardness(η)	1.822	1.129
Chemical potential(μ)	-5.104	-4.046
Electrophilicity index(ω)	7.148	7.247
Chemical softness(s)	0.549	0.885

3.5 Dipole moments

Dipole moment is an important parameter in structural chemistry, and it can be used as a descriptor to illustrate the charge transfer through the molecule. The direction of the dipole moment vector in a molecule depends on the centers of positive and negative charges. The dipole moment for chalcone and pyrazoline are calculated as 5.6792 D and 4.7789 D respectively for B3LYP level. The polarizability (α_0) and first-order hyperpolarizability (β_{tot}) are related directly to the non-linear optical efficiency of structures. The calculated values of α_0, β_{tot} by the finite field approach are given in **Table 4**. The electron-withdrawing substituent like NO_2 group in chalcone and pyrazoline are increased the β_{tot} values.

The transfer of π-electron from electron donating methyl group to the electron withdrawing nitro group makes the molecule as highly polarizable. Accordingly, intramolecular charge transfer interactions may be responsible for the NLO properties. NLO properties get enhanced by the substitution of molecule with carbonyl and nitro group which are involved in hydrogen bond interactions [40]. It is believed that this type of hydrogen bonding is the main source of non-linear crystal like urea (μ and β of urea are 1.3732 Debye and 0.3728×10^{-30}esu) [41]. The mean polarizability value was calculated for chalcone and its pyrazoline as 43.63 $x10^{-24}$ and 56.63 $x10^{-24}$ esu, respectively. These values are much higher than that of *para*-nitro-aniline (pNA) molecule which is a typical NLO material [42, 43]. The hyperpolarizability value was calculated as 33.79 x 10^{-30} esu and 29.21 x 10^{-30} esu for chalcone and pyrazoline in B3LYP level.

Table-4 : Dipole moments and hyperpolarizabilities by DFT method

Parameters	**Symbol**	**Chalcone**	**Pyrazoline**
Dipole moment	μ_{total}	5.6792 D	4.7789 D
Hyperpolarizability	β_0	33.79 $x10^{-30}$esu	29.21 $x10^{-30}$esu
Polarizabilty	α_0	43.63 x 10^{-24}esu	56.63 $x10^{-24}$esu

3.6. Molecular surfaces

Molecular electrostatic potential (MEP) for a molecule gives information about the presence of intra- and intermolecular interactions, predicts the reactive sites and relative reactivities towards electrophilic attack. It also provides a visual method to understand the relative polarity of the molecule. MEPs were calculated at the B3LYP/6-31G (d,p) level to predict reactive sites for electrophilic and nucleophilic attacks of compounds 1 and 2. The negative regions (red and yellow) of the MEP are associated with electrophilic reactivity, while the positive (blue) region is associated with nucleophilic reactivity. For clarity, the color of the MEP surface is as follows: red, electron-rich, partially negatively charged; blue indicates electron deficient, partially positively charged; blue light is somewhat electronless; Yellow is somewhat electron rich area; green to medium respectively. As can be seen from **Figure 5**, the negative sites are mainly oxygen atoms of nitro and carbonyl groups, indicating that electrophilic attack sites may exist. The largest positive site is on the hydrogen of the H-C=C-H group, indicating a potential site for nucleophilic attack. These sites provide information about regions where the compound can cause intermolecular interaction. Therefore, in chalcone, the existence of intermolecular C-H- - -O interactions observed in the solid state. In case of pyrazoline, the nitrogen and oxygen atoms of nitro groups are good electrophilic site.

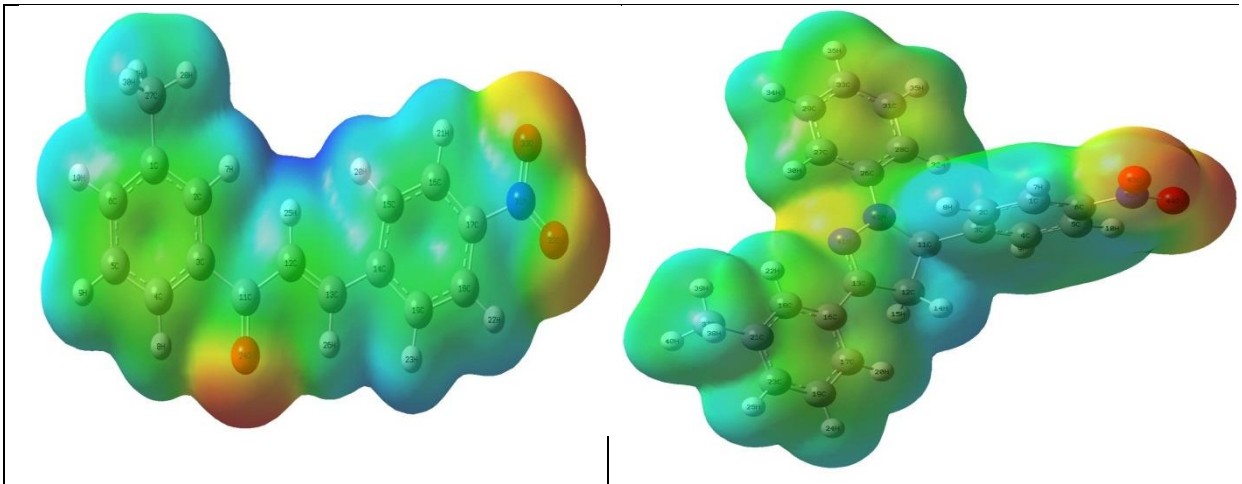

Chalcone (**1**) | Pyrazoline (**2**)

Figure-5 : MEP diagram of compounds **1** and **2**

3.7 Mulliken atomic charges

Mulliken atomic charges are calculated and reported in **Table 5**. Mulliken atomic charge calculation has an important role in the application of quantum chemical calculations [44, 45]. As indicated in **Table 5**, carbonyl carbon C11 (0.229) and nitro substituted carbon C17 (0.321) atoms carries the largest positive charges among the other carbon atoms, therefore, expected to be the site for nucleophilic attack in the chalcone compound. In case of pyrazoline, the nitro group substituted carbon C6 (0.232) and carbon C26 (0.228) attached to pyrazoline N atom have shown larger positive values which are active nucloephilic sites. The oxygen atoms attached with carbonyl group O26 (-0.443), nitro group oxygens of O32 (-0.290) and O33 (-0.291) have shown largest negative charges in chalcones and pyrazoline nitrogens N41 (-0.232), N42 (-0.471) and nitro group oxygens O43 (-0.225) and O44 (-0.226) have shown largest negative charges. These negative charges evidenced that these sites are good electrophilic sites. These are charted and displayed in **Fig. 6**.

Table-5 : Mulliken atomic charges of compounds **1** and 2

Chalcone (1)					**Pyrazoline (2)**			
Atom	**Charge**	**Atom**	**Charge**		**Atom**	**Charge**	**Atom**	**Charge**
1C	0.100	15C	-0.006		2 C	0.019	19 C	-0.007
2C	-0.032	16C	0.073		3 C	0.148	21 C	0.083
3C	0.042	17C	0.321		4 C	-0.024	23 C	-0.013
4C	0.037	18C	0.079		5 C	0.103	26 C	0.228
5C	0.003	19C	-0.030		6 C	0.232	27 C	0.038
6C	-0.004	24O	-0.443		11 C	0.048	28 C	0.034
11C	0.229	27C	-0.019		12 C	0.037	29 C	-0.008
12C	0.029	31N	0.048		13 C	0.146	31 C	-0.012
13C	0.037	32O	-0.290		16 C	0.109	33 C	0.020
14C	0.118	33O	-0.291		17 C	-0.040	37 C	-0.008
					18 C	-0.016		

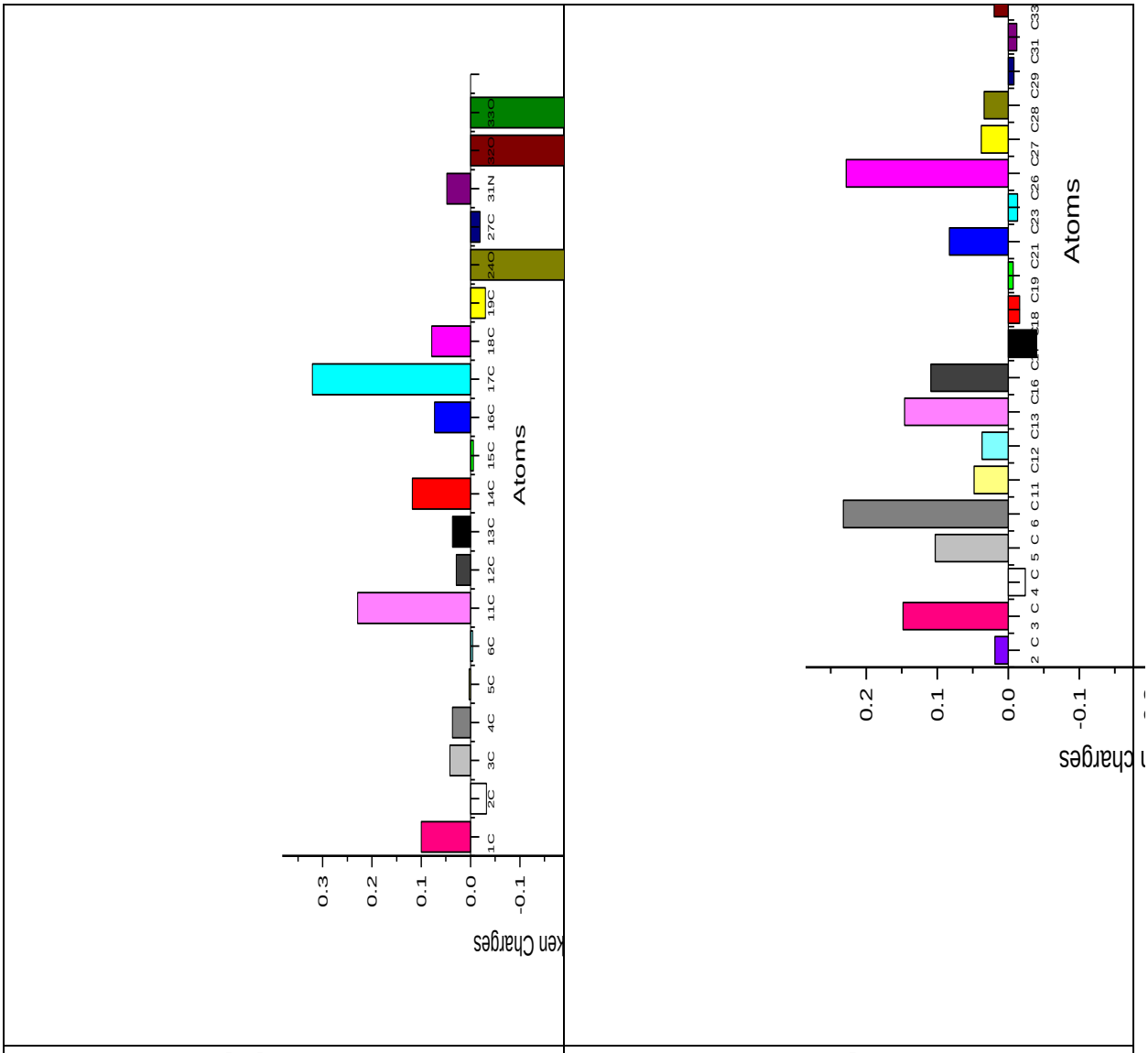

Chalcone (1) **Pyrazoline (2)**

Figure-6 : Chart of mulliken charges by DFT method for **1** and **2**

3.8 Antimicrobial activities of the synthesized compound

The synthesized compounds chalcone and its pyrazoline derivative were screened for its in- vitro antibacterial properties are effective against pathogenic bacteria such as *Staphylococcus aureus, Bacillus subtilis*, *Escherichia coli* and *Salmonella typhi* and three fungi *Aspergillus niger*, *Aspergillus flavus* and *Candida albicans*. The activity of compounds **1** and **2** was tested using the agar diffusion method [46]. Penicillin (25 µg/mL) was used as antibiotic and nystatin (25 µg/mL) was used for prophylaxis. Dimethyl sulfoxide (1% DMSO) was used as a control, e.g., no compound. Bacteria were grown on nutrient agar slants at 37 ± 0.5°C for 24 hours. Use inoculum with 0.1 mL of sterile saline (0.1 mL). Then 85% of 105 CFU/mL 0.1 mL of compound solution at a concentration of 25-150 µg/mL was added to each species in a 6 mm diameter well. All plates were incubated at 37 ± 0.5°C for 24 hours. Record the zone of inhibition (mm) of the compound and record the minimum inhibition concentration (MIC). For immunity, all fungal cultures were maintained on potato

dextrose agar (PDA) at a slope of 27 ± 0.2 for 24-48 hours until sporulation. Transfer the spores of the strain to 5 mL of sterile distilled water containing 1% Tween-80 (to properly remove the spores). Spores were counted with a hemocytometer (106 CFU/mL). Prepare sterile PDA plates containing 2% agar, spread 0.1 mL of each fungal spore suspension on each plate and incubate for 12 hours at 27 ± 0.2 °C. After incubation, use a sterile punch to make an adequate preparation, fill each agar well with 0.1 mL of compound solution at a concentration of 25 to 150 µg/mL. Keep the plate in the refrigerator for 20 minutes to allow diffusion, and then incubate for 24-28 hours at 27 ± 0.2 °C. After incubation, the zone of inhibition of the compound is measured in mm and the standard and minimum inhibition concentration (MIC) are recorded. The results of the antibiotic are given in **Table 6**. From the results of antibiotic data, this drug has been shown to have good activity against *E. coli*.

The titled compounds have shown moderate activity against some other bacterial and fungal species as compared to standard.

Table-6: Antimicrobial activities of compounds **1** and **2**

Compounds	Bacterial species				Fungal species		
	E. coli	**B. subtilis**	**Streptococcus**	**S.typhi**	**A. niger**	**A. flavus**	**C. albicans**
1	16	15	14	16	13	11	15
2	15	12	12	15	10	8	13
Standard	18 (25)	16 (25)	18 (25)	21 (25)	16 (25)	15 (25)	18 (25)

Zone of inhibition was expressed in mm, MIC values (mg/mL) are given in brackets, MIC>50mg L^{-1}. DMSO was used as solvent.

3.9 Anti-inflammatory activity of synthesized derivatives using HRBC assay

Fresh human blood was drawn and mixed with equal parts sterilised Alsever's solution (Dextrose 2%, Sodium citrate 0.8%, Citric acid 0.05%, Sodium chloride 0.42%, and Distilled water 100mL). This blood solution was centrifuged for 10 minutes at 3000 rpm before being washed three times with an equal volume of normal saline. The blood volume is measured and reconstituted as a 10% v/v suspension with normal saline. The reaction mixture, which included 1.0mL of test sample at various concentrations in normal saline and 0.5mL of 10% HRBC suspension, 1mL of 0.2M phosphate buffer, and 1mL hyposaline, was incubated at 37°C for 30 minutes and centrifuged at 3,000 rpm for 30 minutes. The supernatant solution's haemoglobin content was determined spectrophotometrically at 560nm. Each experiment was carried out three times. In this study, dichlorofenac sodium was used as the standard and distilled water as the control. Where the blood control represents either 100% hemolysis or 0% stability, the percentage of HRBC hemolysis calculated by formula [47].

The in-vitro anti-inflammatory activity revealed that the chalcone derivatives exhibited significant activity when compared to the standard, diclofenac sodium. **Table 7** shows the percentage of anti-inflammatory activity of chalcone and its pyrazoline derivative. All inhibitors offered adequate protection in a dose-dependent manner. Due to the resemblance of RBC membrane with the lysosomal membrane, it may possibly inhibit the release of the lysosomal contents of neutrophils at the site of inflammatory reactions. Such

neutrophil lysosomal constituents include bactericidal enzymes and proteases, which upon extracellular release cause further inflammation and tissue damage. At 500µg/ml, the highest effect of stabilization was presented by compound **1** with 83.65% protection. But the compound **2** showed 79.56 %. At the lowest concentration (100µg/mL.), same pattern was observed. These results may be due to prevention of chemical mediator-release or stabilization of the human RBC membrane properties which could be attributed to the inhibition of hypotonicity-induced lysis of membrane [48]. Additionally, it may be assumed that anti-oxidant and radical scavenging activities of the chalcone play a key role in preventing human RBC membrane [49]. However, the anti-inflammatory activity was found to be lower than that of diclofenac sodium (85.76%) for chalcone and its derivatives. Although the precise mechanism of membrane protection action is not deciphered by this study, it may be assumed that the inhibitory compound might mediate membrane protection action by changing its surface area/volume ratio of the cells leading to an increase in the membrane dimensions or shrinking of the cells or by interactions with the membrane proteins [50].

Table-7 : IC50 values of the compounds 1 and 2 calculated based on HRBC membrane stabilization assay

Compounds	Concentration (µg/ml)	% of inhibition	IC50
1	100	28.46	143.86
	250	57.84	
	500	83.65	
2	100	32.46	167.42
	250	56.18	
	500	79.56	

In-vitro anti-inflammatory activity of chalcone and its derivative by HRBC method showed IC50 value greater than 100µg/ml. whereas the IC50 value of compound **1** was calculated to be 143.86 µg/ml. Out of these two compounds, compound **1** has showed the minimum IC50 value. The observed IC50 value showed that compound **1** exhibited highest anti-inflammatory activity. Compounds **2** showed maximum percentage inhibition of 79.56% at the concentration of 500µg/ml which is comparable with that of standard drug diclofenac sodium which showed the percentage inhibition of 86.61% at the concentration of 500µg/ml.

4. Conclusion

In the present study, a chalcone (1) and its cyclic derivative (2) have been synthesized by sing ultrasonic energy in order to lesser time when compared to conventional methods. The formation of these compounds is confirmed by their spectral data. The DFT studies were calculated using Guassian 09W programme. From this calculation, the geometrical parameter, Molecular orbital energies, MEP analysis and Mulliken charges were calculated. HOMO-LUMO energy gap said that compound (**1**) is more reactive and soft than compound (**2**). The dipole moments also revealed that compounds (1) has good NLO property. The

antibacterial screening showed better activities than fungal pecies. The anti-inflammatory activity also showed better results.

Credit to authorship contribution statement

S. Prabha : Investigation, Supervision, Conceptualization, Methodology, Validation, Writing - review & editing

Declaration of Competing Interest

The author declare that they have no known competing financial interests or personal relationships that could have appeared to influence the work reported in this paper.

Acknowledgement:

The author thank to the Department of Chemistry, Govt. Arts College, Chidambaram for providing research facilities for doing this work.

Reference:

[1] K. Damodar, J.K. Kim, J.G. Jun, Synthesis and pharmacological properties of naturally occurring prenylated and pyranochalcones as potent anti-inflammatory agents. Chin. Chem. Lett. 27 (2016) 698-702, https://doi.org/10.1016/j.cclet.2016.01.043

[2] S. Vembu, S. Pazhamalai, M. Gopalakrishnan, Synthesis, spectral characterization, and effective antifungal evaluation of 1H-tetrazole containing 1,3,5-triazine dendrimers. Med. Chem. Res. 25 (2016) 1916–1924, https://doi.org/10.1007/s00044-016-1627-6

[3] P.M. Sivakumar, T.M. Kumar, M. Doble, Antifungal activity, mechanism and QSAR studies on chalcones. Chem. Biol. Drug Des. 74 (2009) 68–79, https://doi.org/10.1111/j.1747-0285.2009.00828.x

[4] J. Muškinja, A. Burmudžija, Z. Ratkovi´c, B. Rankovi´c, M. Kosani´c, G.A. Bogdanovi´c, S.B. Novakovi´c, Ferrocenyl chalcones with O-alkylated vanillins: Synthesis, spectral characterization, microbiological evaluation, and single-crystal X-ray analysis, Med. Chem. Res. 25 (2016) 1744–1753, https://doi.org/10.1007/s00044-016-1609-8

[5] G. Mazzone, A. Galano, J.R. Alvarez-Idaboy, N. Russo, Coumarin-chalcone hybrids as peroxyl radical scavengers: Kinetics and mechanisms, J. Chem. Inf. Model. 56 (2016) 662–670, https://doi.org/10.1021/acs.jcim.6b00006

[6] N. Tadigoppula, V. Korthikunta, S. Gupta, P. Kancharla, T. Khaliq, A. Soni, R.K. Srivastava, K. Srivastava, S.K. Puri, K.S.R Raju, Synthesis and insight into the structure-activity relationships of chalcones as antimalarial agents, J. Med. Chem. 56 (2012) 31–45, https://doi.org/10.1021/jm300588j

[7] N. Sharma, D. Mohanakrishnan, U.K. Sharma, R. Kumar, A.K. Sinha, D. Sahal, Desing, economical synthesis and antiplasmodial evaluation of vanillin derived allylated chalcones and their marked synergism with artemisinin againts chloroquine resistant strains of plasmodium falciparum, Eur. J. Med. Chem. 79 (2014) 350–368, https://doi.org/10.1016/j.ejmech.2014.03.079

[8] R. Pingaew, A. Saekee, P. Mandi, C. Nantasenamat, S. Prachayasittikul, R. Ruchirawat, V. Prachayasittikul, Synthesis, biological evaluation and molecular docking of novel chalcone-coumarin hybrids as anticancer and antimalarial agents, Eur. J. Med. Chem. 85 (2014) 65–76, https://doi.org/10.1016/j.ejmech.2014.07.087

[9] M. Cabrera, M. Simoens, G. Falchi, L. Lavaggi, O.E. Piro, E.E. Castellano, A. Vidal, A. Azquete, A. Monge, A. López, Synthetic chalcones, flavonones, and flavones as antitutumoral agents: Biological and structure-activity relationships, Bioorg. Med. Chem. 15 (2007) 3356–3367, https://doi.org/10.1016/j.bmc.2007.03.031

[10] D. Coskun, B. Gunduz; M.F. Coskun, Synthesis, characterization and significant optoelectronic parameters of 1-(7-methoxy^{-1}-benzofuran-2-yl) substituted chalcone derivatives, J. Mol. Str. 1178 (2019) 261-267, https://doi.org/10.1016/j.molstruc.2018.10.043

[11] H. Hegde, R.K. Sinha, S.D. Kulkarni, S. Nitinkumar, N.S. Shetty, Synthesis, photophysical and DFT studies of naphthyl chalcone and nicotinonitrile derivatives, J. Photochem. & Photobio. Chem. 389A (2020), https://doi.org/10.1016/j.jphotochem.2019.112222

[12] A. Aboelnaga, E. Mansour, A. Hoda, H.M. Ahmed, Synthesis of Asymmetric Pyrazoline Derivatives from Phenylthiophenechalcones; DFT Mechanistic Study, J. Kor. Chem. Soc. 65 (2021), https://doi.org/10.5012/jkcs.2021.65.2.113

[13] G.S.B. Viana, M.A.M. Bandeira, F.J.A. Matos, Analgesic and antiinflammatory effects of chalcones isolated from Myracrodruon urundeuva Allemão, Phytomed. Midicine, 10: (2003) 189-195, https://doi.org/10.1078/094471103321659924

[14] X. Wu, E.R. Tiekink, I. Kostetski, N. Kocherginsky, A.L. Tan, Antiplasmodial activity of ferrocenyl chalcones: investigations into the role of ferrocene, Eur. J. Pharm. Sci. 27 (2006) 175-187, https://doi.org/10.1016/j.ejps.2005.09.007

[15] Y. Luo, R. Song, Y. Li, S. Zhang, Z.J. Liu, Design, synthesis, and biological evaluation of chalcone oxime derivatives as potential immunosuppressive agents, Bioorg. & Med. Chem. Lett., 22 (2012) 3039-3043, https://doi.org/10.1016/j.bmcl.2012.03.080

[16] R.J. Anto, K. Sukumaran, G. Kuttan, M.N.A. Rao, V. Subbaraju, R. Kuttan, Anticancer and antioxidant activity of synthetic chalcones and related compounds, Can. ett. 97(1), 33-37, https://doi.org/10.1016/0304-3835(95)03945-S

[17] M. Swaminathan, S. Kanagarajan, R. Chandrasekaran, A. Sivasubramaniyan, R. raja, P. Alagusundaram, Synthesis, structural, DFT investigations and antibacterial activity assessment of pyrazoline-thiocyanatoethanone derivatives as thymidylate kinase inhibitors, J. Chin. Chem. Soc. (2019) 1-13, DOI: 10.1002/jccs.201900363

[18] R. Guptha, N. Guptha and A. Jain, Improved synthesis of chalcones and pyrazolines under ultrasonic irradiation, Ind. J. Chem. 49B (2010) 351-355.

[19] W.P. Oziminski, J.C. Dobrowolski, σ- and π-electron contributions to the substituent effect: natural population analysis, J. Phys. Org.Chem. 22 (2009) 769, https://doi.org/10.1002/poc.1530

[20] N.P.G. Roeges, (1994) A guide to the complete interpretation of infrared spectra of organic structures. Wiley, New York

[21] D.A. Zainuri, S. Arshad, C.N. Khalib, I.A. Razak, R.R. Pillai, S.F. Sulaiman, N.S. Hashim, K.L. Ooi, S. Armakovic, S.J. Armakovic, C.Y. Panicker, C.V. Alsenoy, Synthesis, XRD crystal structure, spectroscopic characterization (FT-IR, 1H and 13C NMR), DFT studies, chemical reactivity and bond dissociation energy studies using molecular dynamics simulations and evaluation of antimicrobial and antioxidant activities of a novel chalcone derivative, (E)-1-(4-bromophenyl)-3-(4-iodophenyl)prop-2-en-1-one, J. Mol. Struct. 1128 (2017) 520–533, https://doi.org/10.1016/j.molstruc.2016.09.022

[22] S.R. Maidur, P.S. Patil, A. Ekbote, T.S. Chia, C.K. Quah, Molecular structure, second and third-order nonlinear optical properties and DFT studies of a novel non-centrosymmetric chalcone derivative: (2E)-3-(4-fluorophenyl)-1-(4-{[(1E)-(4-fluorophenyl) methylene]amino}phenyl)prop-2-en-1-one. Spectrochim Acta. Mol. Biomol. Spectro. 184A (2017) 342–354, https://doi.org/10.1016/j.saa.2017.05.015

[23] S.K. Mohamed, J.T. Mague, M. Akkurt, M.R. Albayati, A.F. Mohamed, Crystal structure of 1-(2,4-dinitrophenyl)-3,5-diphenyl-1*H*-pyrazole, Acta Cryst E 71(12) (2015) o931-o932, doi: 10.1107/S2056989015021350

[24] T. Dudev, P.B. Parvanova, D. Pencheva, B. Galabov, Molecular geometry, vibrational frequencies, infrared intensities and C N effective bond charges in a series of simple nitrile compounds: HF/6-3 lþG(d,p) molecular orbital study, J. Mol. Struct. 427 (1997) 436–437, https://doi.org/10.1016/S0022-2860(97)00140-3

[25] A.N. Prabhu, A. Jayarama, K. Subrahmanya Bhat, V. Upadhyaya, Growth, characterization and structural investigation of a novel nonlinear optical crystal, J. Mol. Struct. 79 (2013) 1031, https://doi.org/10.1016/j.molstruc.2012.06.057

[26] G. Varsanyi, (1974) Assignments of the spectra of 700 benzene derivative. Academic Press, New York

[27] N.B. Colthup, L.H. Daly, S.E. Wimberly, (1990) Introduction to infrared & Raman spectroscopy. Academic Press, New York.

[28] S. Nayak, V. Poral, G. Hari, K.S.R. Pai, R.K. Sinha, N.K. Lokanath, S.R.G. Naraharisetty, S.L. Goankar, Synthesis, Crystal Structure, Biological Evaluation, DFT Calculations and Third Order Nonlinear Optical Studies of Pyrazolines, J. Mol. Struct. 1243 (2021) 130780, https://doi.org/10.1016/j.molstruc.2021.130780

[29] S. Arshad, D.A. Zainuri, N.C. Khalib, K. Thanigaimani, M.M. Rosil, I.A. Razak, S.F. Sulaiman, N.S. Hashim, K.L. Ooi, Structure, spectroscopic properties and theoretical studies of (E) -1-(4-bromophenyl)-3-(2,3,4-trimethoxyphenyl) prop-2-en-1-one as a potential anti-oxidant agent, Mol. Cryst. Liq. Cryst. 664(1) (2018) 218–240, https://doi.org/10.1080/15421406.2018.1473081

[30] N. Udaya Sri, K. Chaitanya, M.V.S. Prasad, V. Veeraiah, A. Veeraiah, Experimental (FT-IR, FT-Raman and UV-Vis spectra) and density functional theory calculations of diethyl 1Hpyrazole-3,5-dicarboxylate, J. Mol. Struct. 1019 (20212) 68, https://doi.org/10.1016/j.molstruc.2012.03.032

[31] M. Arockia doss, S. Savithiri, G. Rajarajan, V. Thanikachalam, H. Saleem, Synthesis, spectroscopic (FT-IR, FT-Raman, UV and NMR) and computational studies on 3t-pentyl-2r,6c diphenylpiperidin-4-one semicarbazone, Spectrochim Acta. Mol. & Biomol. Spect. 148A (2015) 189, https://doi.org/10.1016/j.saa.2015.03.117

[32] N. Omri, M. Yahyaoui, R. Banani, S. Messaoudi, F. Moussa, M. Abderrabba, *Ab-initio* HF and density functional theory investigations on the synthesis mechanism, conformational stability, molecular structure and UV spectrum of N0-Formylkynurenine, J. Theor. Comput. Chem. 15 (2016) 1650006, https://doi.org/10.1142/S0219633616500061

[33] B. Kosar, C. Albayrak, Spectroscopic investigations and quantum chemical computational study of (*E*)-4-methoxy-2-[(p-tolylimino)methyl]phenol, Spectrochim Acta. Mol. & Biomol. Spect. 78A (2011) 160, https://doi.org/10.1016/j.saa.2010.09.016

[34] R. Mishra, A. Srivastava, A. Sharma, P. Tondon, C. Baraldi, M.C. Gameroni, Structural, electronic, thermodynamical and charge transfer properties of chlorophenicol palmitate using vibrational spectroscopy and DFT calculations, Spectrochem. Acta. Mol. Biomol Spectro. 101A (2013) 335–342. https://doi.org/10.1016/j.saa.2012.09.092.

[35] R.G. Parr, L.V. Szentpaly, S. Liu, Electrophilicity index, J. Am. Chem. Soc. 121 (1999) 1922–01924, doi: 10.1021/ja983494x.

[36] R.G. Parr, R.A. Donnelly, M. Levy and W.E. Palke, Electronegativity: The density functional viewpoint, J. Chem. Phys. 68 (1978) 3801–3807, doi: 10.1021/ja004105d.

[37] P.K. Chattaraj, D.R. Roy, Update 1 of: Electrophilicity index, Chem. Rev. 107 (2007) PR64-PR74. doi: 10.1021/cr078014b.

[38] A. Lesar, I. Milosev, Density functional study of the corrosion inhibition properties of 1,2,4-triazole and its amino derivatives, Chem. Phys. Lett. 483 (2009) 198–203, doi: 10.1016/j.cplett.2009.10.082.

[39] N.R. Sheela, S. Muthu, S. Sampathkrishnan, Molecular orbital studies (hardness, chemical potential and electrophilicity), vibrational investigation and theoretical NBO analysis of 4, 4'-(1H^{-1},2,4-triazol^{-1}-yl methylene) dibenzonitrile based on abinitio and DFT methods, Spectrochim. Acta. Mol. & Biomol. Spect. 120A (2014) 237–251, doi:10.1016/j.saa.2013.10.007

[40] M.K. Marchewka, J. Baran, A. Pietraszko, A. Haznar, S. Debrus, H. Ratajczak, Crystal structure, vibrational spectra and nonlinear optical properties of new melaminium salt: 2,4,6-triamino-1,3,5-triazin-1,3-ium tartrate monohydrate, Solid State Sci. 5(3) (2003) 509-518, https://doi.org/10.1016/S1293-2558(03)00029-3

[41] J.L. Quadar, R. Hierle, J. Appl. Phys. 48 (1977) 2699, https://doi.org/10.1063/1.324120

[42] P. Kaatz, E.A. Donley, D.P. Shelton, J. Chem. Phys. 108 (1998) 849, https://doi.org/10.1063/1.475448

[43] L.T. Cheng, W. Tam, S.H. Stevenson, G.R. Meredith, G. Rikken, S.R. Marder, Experimental investigations of organic molecular nonlinear optical polarizabilities. 1. Methods and results on benzene and stilbene derivatives, J. Phys. Chem. 95(26) (1991) 10631-10643, https://doi.org/10.1021/j100179a026

[44] M. Govindrajan, M. Karabacak, A. Savitha, S. Periandy, FT-IR, FT-Raman, ab-initio HF and DFT study, NBO, HOMO–LUMO and electronic structure calculation on 4-chloro-3-nitrotolune. Spectrochima Acta. Mol. & Biomol. Spectr. 89A (2012) 137–148, https://doi.org/10.1016/j.saa.2011.12.067

[45] S. Gunasekaran, S. Kumaresan, R. Arunbalaji, G. Anand, S. Srinivasan, Density functional theory study of vibrational spectra and assignment of fundamental modes of dacarbazine, J. Chem. Sci. 120(3) (2008) 315–324, https://doi.org/10.1007/s12039-008-0054-8

[46] D. Shrinivasan, N. Sangeetha, T. Suresh, P. Lakshamanperumalsamy, Antimicrobial activity of certain Indian medicinal plants used folkloric medicines, J. Ethnopharmacol. 74 (2001) 217–220, https://doi.org/10.1016/S0378-8741(00)00345-7

[47] Y. Nagaharika, S. Rasheed, Anti-inflammatory activity of leaves of Jatropha gossypifolia L. by HRBC membrane stabilization method, J. Acute Disease, 2 (2013) 156-158, https://doi.org/10.1016/S2221-6189(13)60118-3

[48] P. Padmanabhan, S.N. Jangle, Evaluation of in-vitro anti-inflammatory activity of herbal preparation, a combination of four medicinal plants, Int. J. Basic & Appl. Medical Sci. 2 (2012) 109-116, http://www.cibtech.org/jms.htm 2012 Vol. 2 (1) January-April, pp.109 -116/ Padmanabhan and Jangle

[49] M.A. Kamble, D.K. Mahapatra, D.M. Dhabarde, A.R. Ingole, Pharmacognostic and pharmacological studies of Bombax ceiba thorn extract, J. Pharm. & Pharmacog. Res. 5 (2017) 40-54, http://jppres.com/jppres

[50] N.K. Khadka, (2019) Modulations of Lipid Membranes Caused by Antimicrobial Agents and Helix of Endophilin. 13904626.